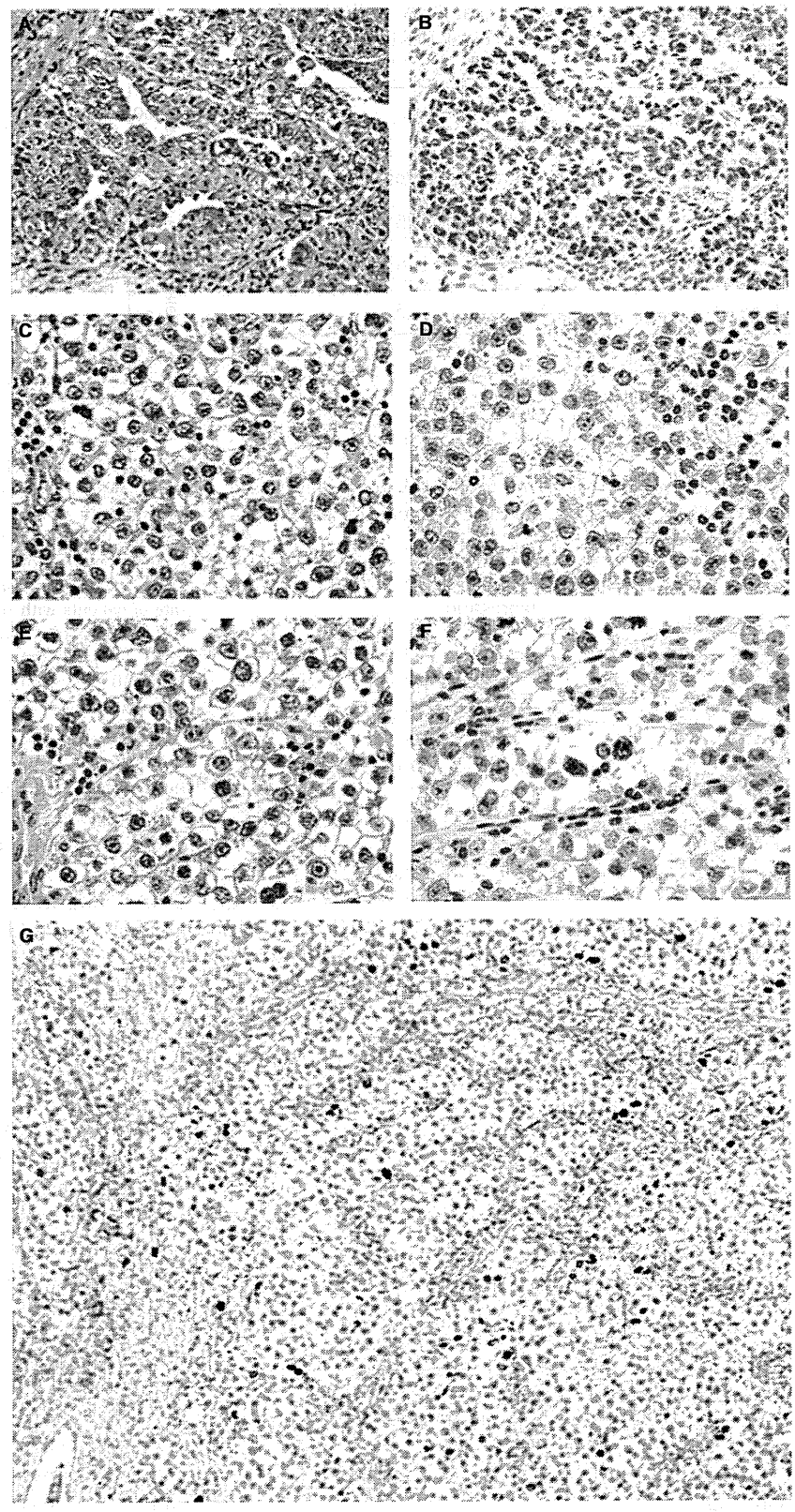

Figure 2. Haematoxylin and eosin staining (A,C,E) and immunohistochemistry with anti-human DNA methyltransferase 3B (DNMT3B) antibody (B,D,F,G) in testicular germ cell tumours. Embryonal carcinomas, as positive controls, showed diffuse and strong nuclear immunoreactivity for DNMT3B (A,B). Fifty-three of 88 seminomas were completely negative for DNMT3B (C,D), and scattered tumour cells with nuclear immunoreactivity were observed in the other 35 seminomas (E,F). DNMT3B-positive cells showed immunoreactivity as strong as that in embryonal carcinoma, whereas the surrounding tumour cells completely lacked immunoreactivity (F). There were no morphological differences between DNMT3B-positive and DNMT3B-negative cells (E,F). Widely scattered nuclear immunoreactivity for DNMT3B was seen at low magnification (G).

Table 1. Correlation between focal DNA methyltransferase 3B (DNMT 3B) expression and initial TNM stage in patients with seminomas

	Focal DNMT3B expression		
Initial TNM stage	Negative	Positive	*P**
Stage I	45	25	0.011
Stage II	8	5	
Stage III	0	5	

*Chi-squared test.

Table 2. Correlations between focal DNA methyltransferase 3B (DNMT3B) expression and clinicopathological parameters in stage I seminomas

	Focal DNMT3B expression		
Clinicopathological parameters	Negative	Positive	*P**
Tumour size (mm)			
≤40	16	8	0.764
>40	29	17	
Invasion of the rete testis†			
Negative	13	10	0.343
Positive	32	15	
Invasion of the epididymis			
Negative	44	24	0.669
Positive	1	1	
Vascular involvement			
Negative	36	15	0.071
Positive	9	10	
Invasion of the spermatic cord			
Negative	44	23	0.253
Positive	1	2	
Tumour relapse			
Negative	42	19	**0.037**
Positive	3	6	

*Chi-squared test.
†All positive cases showed interstitial invasion but not Pagetoid spread.
The *P*-value of <0.05, which indicates significant differences, is in bold.

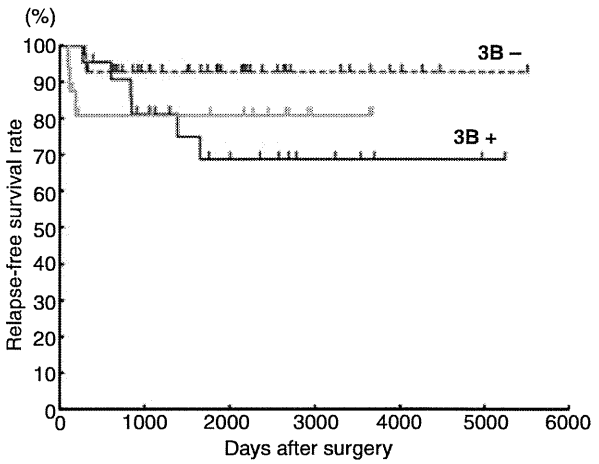

Figure 3. Kaplan–Meier survival curves of patients with stage I testicular germ cell tumours (TGCTs). The relapse-free survival rate of patients with seminomas showing focal DNMT3B expression (red solid line) was significantly lower than that of patients with seminomas not showing this feature (red broken line, $P = 0.0464$). There was no significant difference between the relapse-free survival rate of patients with seminomas showing focal DNMT3B expression and that of patients with non-seminomatous TGCTs (gray line, $P = 0.747$). The time to relapse of patients with seminomas showing DNMT3B expression tended to be longer than that of patients with non-seminomatous TGCTs.

marker for prognostication of patients with seminoma has yet been identified.

In the present study, we found, using immunohistochemistry, that seminomas were separable into two groups on the basis of DNMT3B protein expression: focal DNMT3B expression with widely scattered nuclear reactivity, and absence of such expression. Patients with seminomas showing focal DNMT3B expression were frequently diagnosed at a higher stage (Table 1), and had a poorer outcome (Figure 3), than patients with seminomas lacking such expression.

Tickoo *et al.*[21] suggested that seminomas with 'atypical features', based on morphology, positive expression of CAM5.2 and/or CD30, and negative expression of CD117, tended to be more aggressive, with a higher initial tumour stage. When our cohort of seminomas was examined on the basis of the same methods and criteria,[21] CAM5.2 reactivity (15/87 cases, 17.2%) was significantly correlated with widely scattered nuclear reactivity for DNMT3B ($P = 0.0028$), whereas histological atypia ($P = 0.321$) and expression of CD30 ($P = 0.0653$) and CD117 ($P = 0.0814$) did not show such significant correlations. CAM5.2 reactivity did not correlate significantly with any of the clinicopathological parameters in Table 2, including tumour relapse ($P = 0.949$) or relapse-free survival rate ($P = 0.6300$, log-rank test).

The relapse-free survival rate of patients with seminomas showing focal DNMT3B expression was as low as that of the 16 examined patients with stage I non-seminomatous TGCTs who underwent orchiectomy at the NCCH, Tokyo, Japan ($P = 0.747$; Figure 3), although previously patients with seminomas have been generally considered to have a more favourable outcome than those with non-seminomatous TGCTs.[22,23] Moreover, seminomas showing DNMT3B expression tended to relapse later than non-seminomatous TGCTs (Figure 3). These data indicate that DNMT3B expression may be a potentially useful indicator for estimation of relapse risk in patients with stage I seminoma: patients whose tumours show such expression should be followed up as closely as, and for a longer period than, patients with non-seminomatous TGCTs.

Immunohistochemistry may be the only method capable of detecting widely scattered nuclear reactivity: analyses of mRNA and protein in tissue and serum samples using other methods may not be able to demonstrate DNMT3B expression in only a small number of scattered tumour cells. Thus, immunohistochemistry for DNMT3B, which can be performed on the formalin-fixed, paraffin-embedded tissue specimens prepared for routine pathological diagnosis, may be clinically useful for prognostication of stage I seminomas after prospective validation.

According to the histogenetic model proposed by Srigley *et al.*,[24] seminoma has the potential to differentiate to embryonal carcinoma or other non-seminomatous TGCTs, resembling the differentiation of fertilized germ cells to embryos. In fact, in patients with testicular seminomas who suffer relapse, the metastatic lesions show histological subtypes of embryonal carcinomas and other non-seminomatous TGCTs. *De-novo* DNMT, Dnmt3b, contributes to dynamic epigenetic reprogramming, especially in early mammalian embryogenesis,[10] and is expressed in pluripotent cells, such as the inner cell mass and embryonic ectoderm cells of mouse embryos, and in isolated embryonic stem cells.[25] Embryonal carcinomas also showed high-level expression of DNMT3B (Figure 2A,B).[11,14,15] DNMT3B may be associated with cell pluripotency through its *de-novo* DNA methylation ability, not only during development but also in TGCTs. Focal DNMT3B expression may reflect the potential for differentiation to embryonal carcinomas and other non-seminomatous TGCTs in a proportion of tumour cells in stage I seminoma. It is feasible that seminomas with such potential would relapse as frequently as non-seminomatous TGCTs after a period long enough to allow such differentiation to occur.

References

1. von der Maase H, Specht L, Jacobsen GK *et al.* Surveillance following orchidectomy for stage I seminoma of the testis. *Eur. J. Cancer* 1993; **14**; 1931–1934.
2. NCCN clinical practice guidelines in oncology, testicular cancer, Version 2.2011. Available at: http://www.nccn.org/professionals/physician_gls/f_guidelines.asp
3. Huddart RA, Norman A, Shahibi M *et al.* Cardiovascular disease as a long-term complication of treatment for testicular cancer. *J. Clin. Oncol.* 2003; **21**; 1513–1523.
4. Moller H, Mellemgaard A, Jacobsen GK *et al.* Incidence of second primary cancer following testicular cancer. *Eur. J. Cancer* 1993; **29A**; 672–676.
5. van Leeuwen F, Stiggelbout AM, van den Belt-Dusebout AW *et al.* Second cancer risk following testicular cancer: a follow-up study of 1,909 patients. *J. Clin. Oncol.* 1993; **11**; 415–424.
6. Oliver RT, Mason MD, Mead GM *et al.* MRC TE19 collaborators and the EORTC 30982 collaborators. Radiotherapy versus single-dose carboplatin in adjuvant treatment of stage I seminoma: a randomized trial. *Lancet* 2005; **366**; 293–300.
7. Kanai Y. Genome-wide DNA methylation profiles in precancerous conditions and cancers. *Cancer Sci.* 2010; **101**; 36–45.
8. De Jong J, Weeda S, Gillis AJ *et al.* Differential methylation of the OCT3/4 upstream region in primary human testicular germ cell tumors. *Oncol. Rep.* 2007; **18**; 127–132.
9. Netto GJ, Nakai Y, Nakayama M *et al.* Global DNA hypomethylation in intratubular germ cell neoplasia and seminoma, but not in nonseminomatous male germ cell tumors. *Mod. Pathol.* 2008; **21**; 1337–1344.
10. Okano M, Bell DW, Haber DA *et al.* DNA methyltransferases Dnmt3a and Dnmt3b are essential for *de novo* methylation and mammalian development. *Cell* 1999; **99**; 247–257.
11. Beyrouthy MJ, Garner KM, Hever MP *et al.* High DNA methyltransferase 3B expression mediates 5-aza-deoxycytidine hypersensitivity in testicular germ cell tumors. *Cancer Res.* 2009; **69**; 9360–9366.
12. Woodward PJ, Mostfi FK, Talerman A *et al.* Germ cell tumors. In Eble JN, Sauter G, Epstein J, Sesterhenn IA eds. *World Health Organization classification of tumours. pathology and genetics of tumours of the urinary system and male genital organs.* Lyon: IARC Press, 2004; 221–249.
13. Teshima S, Shimosato Y, Hirohashi S *et al.* Four new human germ cell lines. *Lab. Invest.* 1988; **59**; 328–336.
14. Almstrup K, Hoei-Hansen CE, Nielsen JE *et al.* Genome-wide gene expression profiling of testicular carcinoma in situ progression into overt tumours. *Br. J. Cancer* 2005; **92**; 1934–1941.
15. Biermann K, Heukamp LC, Steger K *et al.* Genome-wide expression profiling reveals new insights into pathogenesis and progression of testicular germ cell tumors. *Cancer Genom. Proteom.* 2007; **4**; 359–367.
16. Chung P, Warde P. Surveillance in stage I testicular seminoma. *Urol. Oncol.* 2006; **24**; 75–79.
17. Pectasides D, Pectasides E, Constantinidou A *et al.* Stage I testicular seminoma: management and controversies. *Crit. Rev. Oncol. Hematol.* 2009; **71**; 22–28.
18. Horwich A, Alsanjari N, A'Hern R *et al.* Surveillance following orchidectomy for stage I testicular seminoma. *Br. J. Cancer* 1992; **65**; 775–778.
19. Warde P, Gospodarowicz M, Banerjee D *et al.* Prognostic factors for relapse in stage I testicular seminoma treated with surveillance. *J. Urol.* 1997; **157**; 1705–1709.

20. Warde P, Specht L, Horwich A *et al.* Prognostic factors for relapse in stage I seminoma managed by surveillance: a pooled analysis. *J. Clin. Oncol.* 2002; **20;** 4448–4452.
21. Tickoo SK, Hutchinson B, Bacik J *et al.* Testicular seminoma: a clinicopathologic and immunohistochemical study of 105 cases with special reference to seminomas with atypical features. *Int. J. Surg. Pathol.* 2002; **10;** 23–32.
22. Jones RH, Vasey PA. Testicular cancer-management of early disease. *Lancet Oncol.* 2003; **4;** 730–737.
23. Bahrami A, Ro JY, Ayala AG. An overview of testicular germ cell tumors. *Arch. Pathol. Lab. Med.* 2007; **131;** 1267–1280.
24. Srigley JR, Mackay B, Toth P *et al.* The ultrastructure and histogenesis of male germ neoplasia with emphasis on seminoma with early carcinomatous features. *Ultrastruct. Pathol.* 1988; **12;** 67–86.
25. Watanabe D, Suetake I, Tada T *et al.* Stage- and cell-specific expression of Dnmt3a and Dnmt3b during embryogenesis. *Mech. Dev.* 2002; **118;** 187–190.

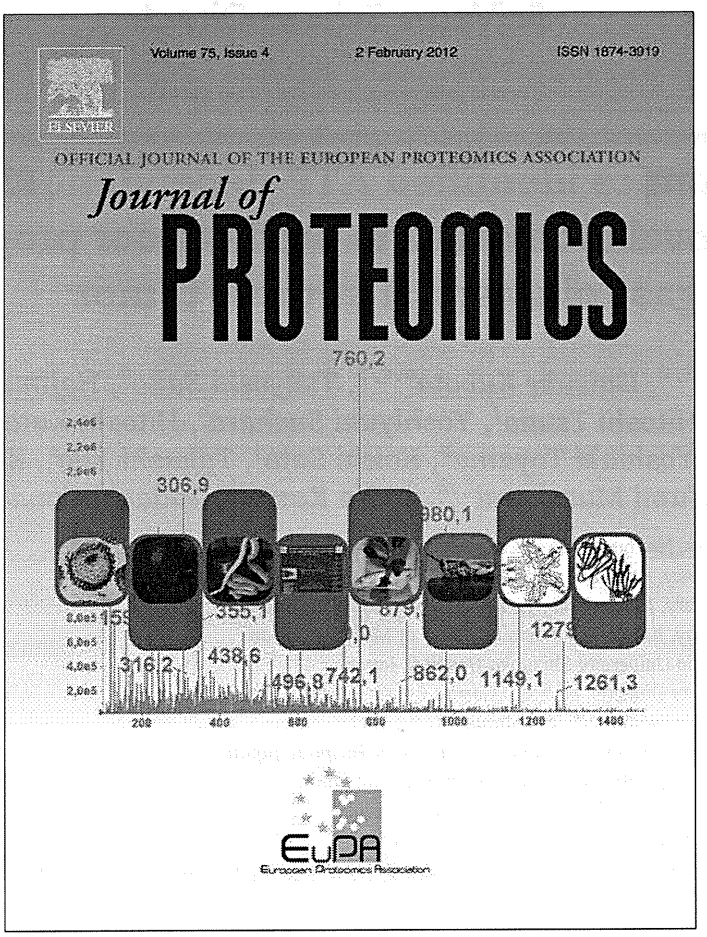

JOURNAL OF PROTEOMICS 75 (2012) 1089–1098

Available online at www.sciencedirect.com

SciVerse ScienceDirect

www.elsevier.com/locate/jprot

Clinical proteomics identified ATP-dependent RNA helicase DDX39 as a novel biomarker to predict poor prognosis of patients with gastrointestinal stromal tumor

Kazutaka Kikuta[a,b,1,2], *Daisuke Kubota*[a,c,1], *Tsuyoshi Saito*[d], *Hajime Orita*[e], *Akihiko Yoshida*[f,g], *Hitoshi Tsuda*[f], *Yoshiyuki Suehara*[c], *Hitoshi Katai*[h], *Yasuhiro Shimada*[i], *Yoshiaki Toyama*[b], *Koichi Sato*[j], *Takashi Yao*[d], *Kazuo Kaneko*[c], *Yasuo Beppu*[k], *Yasufumi Murakami*[l,m], *Akira Kawai*[k], *Tadashi Kondo*[a,*]

[a]*Division of Pharmacoproteomics, National Cancer Center Research Institute, Japan*
[b]*Department of Orthopedic Surgery, Keio University School of Medicine, Japan*
[c]*Department of Orthopedic Surgery, Juntendo University School of Medicine, Japan*
[d]*Department of Human Pathology, Juntendo University School of Medicine, Japan*
[e]*Department of Surgery, Juntendo University Shizuoka Hospital, Japan*
[f]*Pathology and Clinical Laboratory Division, National Cancer Center Hospital, Japan*
[g]*Department of Pathology, The University of Tokyo, Japan*
[h]*Department of Surgical Oncology Division, National Cancer Center Hospital, Japan*
[i]*Gastrointestinal Oncology Division, National Cancer Center Hospital, Japan*
[j]*Department of Surgery, Juntendo University Shizuoka Hospital, Japan*
[k]*Orthopedic Surgery Division, National Cancer Center Hospital, Japan*
[l]*Laboratory of Genome Biology, Department of Biological Science & Technology, Tokyo University of Science, Japan*
[m]*BioMatrix Research Institute, Japan*

ARTICLE INFO

Article history:
Received 30 August 2011
Accepted 8 October 2011
Available online 25 October 2011

Keywords:
ATP-dependent RNA helicase DDX39
Biomarker
2D-DIGE
Gastrointestinal stromal tumor
Prognosis

ABSTRACT

Gastrointestinal stromal tumor (GIST) is the most common mesenchymal malignancy of the gastrointestinal tract, comprising a wide spectrum from a curable disorder to highly malignant disease. GIST is characterized by tyrosine kinase mutations, and molecular targeting therapies against these abnormal enzymes require prognostic biomarkers. To identify candidate prognostic biomarkers, we examined proteomic features corresponding to metastasis after surgery. Using two-dimensional difference gel electrophoresis with a large format gel, we compared the primary tumor tissues of GIST patients free of metastasis for two years after surgery (eight cases) with those of patients who developed metastasis within one year after surgery (nine cases). We found the intensities of 38 protein spots to differ significantly between the two groups. Mass spectrometric protein identification revealed that these corresponded to 25 unique genes. Immunohistochemical validation demonstrated ATP-dependent RNA helicase DDX39 to be significantly associated with metastasis and poor clinical outcomes in a group of 72 GIST patients. In conclusion, we have established a novel prognostic utility of ATP-dependent RNA helicase DDX39 in

* *Corresponding author at:* Division of Pharmacoproteomics, National Cancer Center Research Institute, 5-1-1 Tsukiji, Chuo-ku, Tokyo 104-0045, Japan. Tel.: +81 3 3542 2511x3004; fax: +81 3 357 5298.
E-mail address: takondo@ncc.go.jp (T. Kondo).
[1] These persons contributed equally to this study.
[2] Present address: Tachikawa Memorial Hospital, Tokyo, Japan.

1874-3919/$ – see front matter
doi:10.1016/j.jprot.2011.10.005

GIST.ATP-dependent RNA helicase DDX39, a novel biomarker for GIST likely to be associated with metastatic disease, can identify patients likely to benefit from new therapeutic strategies such as tyrosine kinase inhibitors.

1. Introduction

Though rare, gastrointestinal stromal tumor (GIST) is the most common primary mesenchymal malignancy of gastrointestinal tract, with an incidence of approximately 15 per 1,000,000 people [1,2]. The clinical courses of GIST patients range from a curable disorder to highly malignant disease, and the proportion of highly malignant or high-risk GIST is 20–30% of all cases. GIST is characterized by mutations of c-kit and platelet derived growth factor receptor (PDGFR) [3]. Recently, molecular targeting therapy using imatinib mesylate (STI571, Novartis), a tyrosine kinase inhibitor, was proven to be effective for treating GIST patients [3]. However, as 60% to 80%of GIST patients can be cured by surgical resection alone [1,2], only a limited number may require imatinib treatments. Diagnostic modalities which can identify patients with a poor prognosis before treatment are required to optimize these therapeutic strategies. Tumor location and certain molecular aberrations, including those of c-kit, PDGFR, p16 and pfetin, have been found to correlate with patient outcomes or resistance to imatinib treatment [4–9]. However, the clinical utility of these biomarkers has yet to be established.

Herein, using two-dimensional difference gel electrophoresis (2D-DIGE) with a large format electrophoresis device, we compared protein expressions in primary tumors from GIST patients with and without metastasis, and identified protein expressions associated with outcomes. We identified ATP-dependent RNA helicase DDX-39 as a candidate biomarker and validated its prognostic utility in additional cases by employing immunohistochemistry.

2. Materials and methods

2.1. Patients and clinical information

We examined the tumor tissue proteomes of 17 GIST patients who underwent surgery at the National Cancer Center Hospital from October 1977 to December 2005. All these 17 samples lacked PDGFR mutations, and c-kit mutations did not have prognostic significances [9]. We also immunohistochemically examined 72 tumor tissues from GIST patients who underwent surgery at the Juntendo Hospital during the period from 1990 through 2010. All patients underwent resection with curative intent, and were not treated with adjuvant chemotherapy until distant metastasis was detected. Diagnosis was based on the WHO (World Health Organization) classification system for soft-tissue tumors [10], including determination of tumor size, presence of necrosis, differentiation, mitotic rate, MIB-1 index, presence of epithelioid morphology, and CD34 and CD117 expressions. Risk classification was based on tumor size and the MIB-1 index [11]. The data of individual patients are summarized in Supplemental Table 1. This project was approved by the institutional review boards of the National Cancer Center and Juntendo University.

For proteomic comparison, we divided the GIST samples into two groups. Patients with metastasis at diagnosis or who developed metastasis within one year after surgery, and were categorized as the high-risk group based on their histological findings, were defined as having poor-prognosis GISTs (P-GIST) (samples 1–8). Patients who remained metastasis-free for2 years after surgery, and were categorized as the low or intermediate-risk group based on their histological findings, were defined as having good-prognosis GISTs (G-GIST) (samples 9–17). Previous reports have indicated that the low or intermediate-risk GIST patients who did not develop metastasis within two years postoperatively have better outcomes than high-risk GIST patients who developed metastasis within one year after surgery [11].

2.2. Protein expression profiling

Frozen samples were crushed to powder with a CryoPress (Microtech Nichion, Chiba, Japan) under cooling with liquid nitrogen, and treated with urea lysis buffer (6 M urea, 2 M thiourea, 3% CHAPS, 1% Triton X-100). After centrifugation at 15,000 rpm for 30 min, the supernatant was used for protein expression studies.

2D-DIGE was performed as described previously [12–15]. In brief, the internal control sample was prepared by mixing equal amounts of all individual samples. Five micrograms of the internal control sample and another 5 μg of each individual sample were labeled with Cy3 and Cy5, respectively (CyDye DIGE Fluor saturation dye, GE Healthcare Biosciences, Uppsala, Sweden) according to the manufacturer's instructions. These differently labeled protein samples were mixed and separated by 2D-DIGE. The first dimension separation was achieved using IPG DryStrip gels (24 cm length, pI range between 4 and 7, Multiphor II, GE Healthcare Biosciences). The second dimension separation was achieved by SDS-PAGE using a large format gel device and a separation distance of 33 cm (Biocraft, Itabashi, Tokyo, Japan) [15]. The gels were scanned using laser scanners (Tyhoon Trio, GE Healthcare Biosciences) at appropriate wavelengths. For all spots, the intensity of the Cy5 image was normalized by that of the Cy3 image in the identical gel so that gel-to-gel differences were compensated, using SameSpot image software (Non-linear Dynamics, Newcastle, UK).

2.3. Data analysis

All statistical analyses of proteome data, including hierarchical clustering, principal component analysis and the correlation matrix study employing Wilcoxon's test were conducted

using Expressionist software (Genedata, Basel, Switzerland) [15]. Statistical analyses of clinicopathological parameters were carried out using the χ^2 test or Fisher's exact test in cross tables to assess relationships between ATP-dependen RNA helicase DDX39expression and clinicopathological factors. The tumor-specific and disease-free survivals were calculated from the initial resection of the primary tumor until death due to tumor-specific causes or until first evidence of metastasis or recurrence, respectively. All time-to-event endpoints were computed by the Kaplan–Meier method [16]. Patients who died of causes unrelated to GIST were censored at the time of death. Potential prognostic factors were identified by univariate analysis using the log-rank test. Independent prognostic factors were evaluated using Cox's proportional hazards regression [17] model with variables identified as being significant at the univariate level ($p<0.05$). Calculations were carried out using the SPSS software statistical package (SPSS Japan Inc. Tokyo, Japan).

2.4. *Protein identification by mass spectrometry*

Proteins corresponding to the spots of interest were identified by mass spectrometry [15]. In brief, Cy5-labeled proteins separated by 2D-PAGE were recovered by a large spot picker (AsOne, Osaka, Japan), and the proteins were then treated with modified trypsin (Promega, Madison, WI, USA). The trypsin digests were subjected to liquid chromatography coupled with tandem mass spectrometry with a Finnigan LTQ linear ion trap mass spectrometer (Thermo Electron Co., San Jose, CA, USA). Mascot software was used to search for the masses of the peptide ion peaks against the SWISS-PROT database. Proteins with a Mascot score of 35 or more were used for protein identification. When multiple proteins were identified in a single spot, the proteins with the highest number of peptides were regarded as those corresponding to the spot.

2.5. *Western blotting*

Protein samples were separated by SDS-PAGE and subsequently blotted on a nitrocellulose membrane. The membrane was incubated with rabbit polyclonal antibody against ATP-dependent RNA helicase DDX-39 (1:1000 dilution, Gene Way Biotech, San Diego, CA, USA), and then horseradish peroxidase-conjugated secondary antibody (1:1000 dilution, GE Healthcare Biosciences). Western blotting signals were monitored using an enhanced chemiluminescence system (GE Healthcare Biosciences) and LAS 3000 (Fuji film, Tokyo, Japan).

2.6. *Immunohistochemical staining*

Expression of ATP-dependent RNA helicase DDX39 expression was examined immunohistochemically using paraffin-embedded tissues. In brief, 4-μm-thick tissue sections were deparaffinized through xylene and rehydrated with ethanol. Endogenous peroxidase was blocked with 1% H_2O_2 diluted in methanol for 30 min at room temperature. The slides were autoclaved in 10 mmol/L citrate buffer (pH 6.0) at 121 degrees for 30 min and incubated with the antibody against ATP-dependent RNA helicase DDX39 (dilution, 1:15, BMR00389, Bio Matrix Research, Chiba, Japan) at room temperature overnight. Immunostaining was carried out according to the streptavidin–biotin peroxidase method using the Strept ABC Complex/horseradish peroxidase kit (DAKO). Strongly stained cells were defined as those with staining intensity equivalent to or higher than that of lymphocytes. One pathologist (A.Y.) and one clinician (D.K.) reviewed the sections stained with ATP-dependent RNA helicase DDX39 antibody. Both were blinded to the clinical data (age, sex, anatomic site and clinical outcome). In most cases, the differences between positive and negative staining were so obvious that two reviewers had consistent results.

3. Results

2D-DIGE with a large format electrophoresis device generated proteome data consisting of 3260 protein spots (Fig. 1). In our previous report, 2D-DIGE with a smaller electrophoresis device generated 1513 protein spots using the same protein samples of primary GIST tumors [9]. The larger gel obviously generated more protein spots, possibly because the separation performance of gel electrophoresis correlates with separation distance, and the use of a large format gel allows

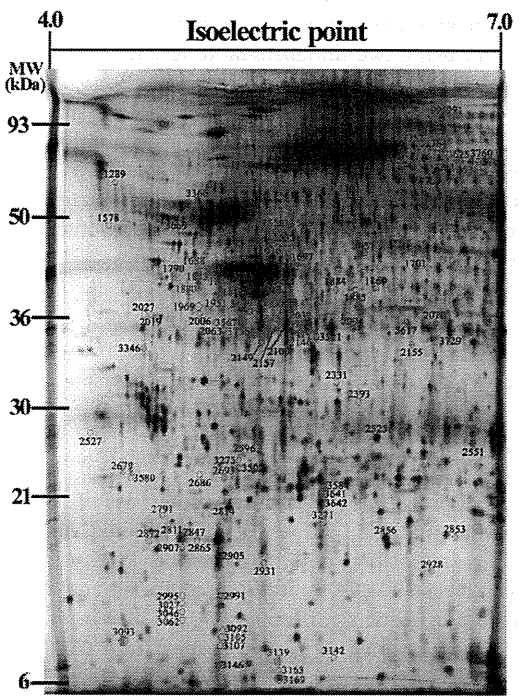

Fig. 1 – Representative 2D image of the primary tumor of a GIST case. The intensity of protein spots marked blue showed a statistically significant difference ($p<0.05$) between the samples from patient groups with different outcomes. The intensity of protein spots marked red showed a statistically significant ($p<0.01$) difference (more than two-fold) between the two groups. The spot numbers correspond to those in Fig. 1 and Table 1.

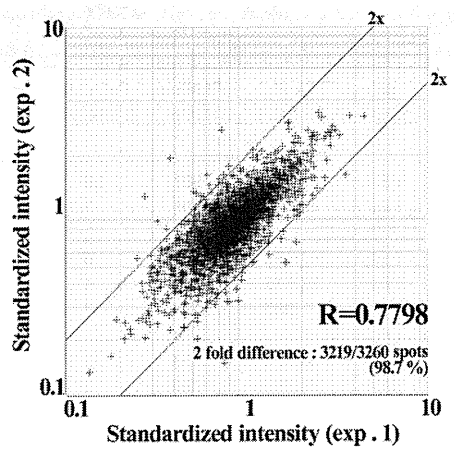

Fig. 2 – System reproducibility was examined by running the same sample three times. The scatter graph demonstrates the high reproducibility of the data obtained by 2D-DIGE.

separation of overlapping protein spots [18]. These issues were extensively discussed as being among the challenges inherent to 2D-PAGE in the previous report [19].

System reproducibility was verified by comparing the protein profiles obtained from two independent separations of the same sample (Fig. 2). Scatter plot analysis revealed that the standardized intensity of 98.7% of the spots ranged within a 2.0-fold difference. Such high reproducibility may be attributable to the use of an internal control sample [20] and a large format gel device [18]. We concluded that system reproducibility was quite acceptable for this protein expression study.

We selected the 38 protein spots with intensities that differed significantly between the sample groups (p value less than 0.01 and more than 2-fold difference). The localizations of these 38 protein spots on the 2D image are demonstrated in Fig. 1, as the protein spots with red numbers, and the differential spot intensities are shown in Fig. 3. In addition to these 38 protein spots, we also detected protein spots differing less significantly between the sample groups ($p<0.05$), and these were marked blue (Fig. 1). Among the 38 protein spots, 11 and 27 had higher intensities in the samples from the G-GIST and P-GIST groups, respectively.

Mass spectrometric protein identification revealed that the 38 protein spots corresponded to 25 distinct gene products (Fig. 3A and Table 1). The samples were grouped according to outcomes based on the intensity of these 38 protein spots

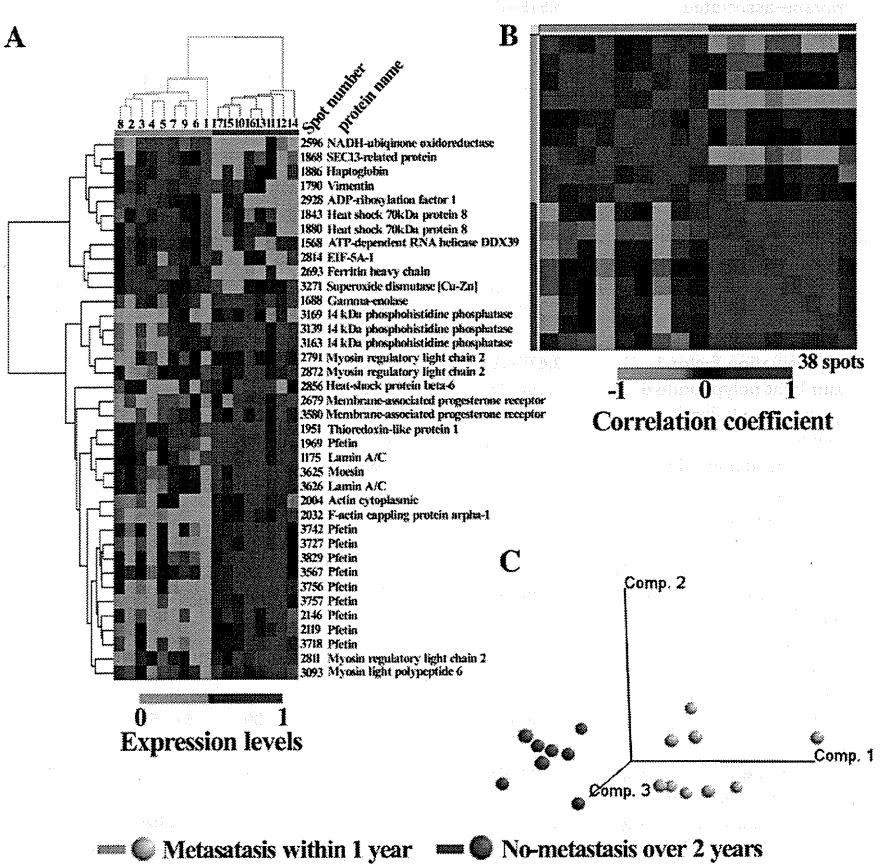

Fig. 3 – The levels of proteins with expressions differing between the patient groups. A. Protein spot intensity is demonstrated as a heat map. B. The correlation matrix demonstrates that the intensities of the 38 protein spots were similar among samples from the same group. C. Principal component analysis showed the sample groups to be clearly separable according to the intensities of the selected protein spots.

Table 1 – List of the proteins with expressions differing between the GIST patient groups with different postoperative outcomes.

Spots No [a]	Accession no [b]	Identified protein [b]	Wilcoxon test p value	Fold difference (ratio of means)	pI (cal) [c]	MW (cal) (kD) [c]	Protein score [d]	Peptide matches	Sequence coverage (%)
1175	P02545	Lamin-A/C	0.001257	2.288	6.57	74,380	581	10	20.3
1568	O00148	ATP-dependent RNA helicase DDX39	8.23E-05	2.211	5.46	49,611	94	2	4.2
1688	P09104	Gamma-enolase	7.90E-03	2.701	4.91	47,450	349	6	13.9
1790	P08670	Vimentin	7.90E-03	2.135	5.06	53,545	201	4	8.8
1843	P11142	Heat shock cognate 71 kDa protein	5.51E-03	2.368	5.37	71,082	138	3	5.4
1868	P55735	SEC13-related protein	7.90E-03	2.240	5.22	35,900	130	2	8.7
1880	P11142	Heat shock cognate 71 kDa protein	1.56E-03	2.544	5.37	71,082	180	3	5.3
1886	P00738	Haptoglobin precursor	1.56E-03	2.427	6.13	45,861	100	2	4.7
1951	O43396	Thioredoxin-like protein 1	3.70E-03	2.037	4.84	32,499	118	4	16
1969	Q96CX2	BTB/POZ domain-containing protein KCTD12 (Pfetin)	3.29E-04	2.555	5.51	35,964	346	8	23.1
2004	P60709	Actin, cytoplasmic 1	7.90E-03	2.131	5.29	42,052	452	12	452
2032	P52907	F-actin capping protein alpha-1 subunit	6.31E-04	3.094	5.45	32,942	286	5	30.5
2119	Q96CX2	BTB/POZ domain-containing protein KCTD12 (Pfetin)	3.29E-04	2.516	5.51	35,964	316	5	20.9
2146	Q96CX2	BTB/POZ domain-containing protein KCTD12 (Pfetin)	9.87E-04	2.560	5.51	35,964	344	8	23.1
2596	P03886	NADH-ubiquinone oxidoreductase	2.47E-03	4.828	6	24,203	162	4	18.1
2679	O00264	Membrane-associated progesterone receptor component 1	5.51E-03	2.130	4.56	21,641	114	3	18.6
2693	P02794	Ferritin heavy chain	5.76E-04	4.296	5.3	21,383	178	4	20.8
2791	P24844	Myosin regulatory light chain 2	3.29E-04	2.022	4.8	19,740	210	4	24.6
2811	P24844	Myosin regulatory light chain 2, smooth muscle isoform	2.47E-03	2.296	4.8	19,740	210	4	24.6
2814	P63241	Eukaryotic translation initiation factor 5A-1	5.51E-03	2.321	5.08	17,049	93	3	26
2856	O14558	Heat-shock protein beta-6	7.90E-03	2.720	5.95	17,182	160	4	23.1
2872	P19105	Myosin regulatory light chain 2	3.70E-03	2.054	4.67	19,707	284	7	30
2928	P84077	ADP-ribosylation factor 1	2.47E-03	2.492	6.36	20,610	252	6	26.7
3093	P60660	Myosin light polypeptide 6	5.23E-03	2.196	4.56	16,959	103	2	14.7
3139	O14737	Programmed cell death protein 5	5.76E-04	4.513	5.78	14,145	107	2	19.4
3163	Q9NRX4	14 kDa phosphohistidine phosphatase	9.87E-04	3.369	5.65	13,995	52	1	8.8
3169	Q9NRX4	14 kDa phosphohistidine phosphatase	3.70E-03	2.779	5.65	13,995	73	2	15.2
3271	P00441	Superoxide dismutase [Cu-Zn]	2.47E-03	2.005	5.7	16,023	84	2	17
3567	Q96CX2	BTB/POZ domain-containing protein KCTD12 (Pfetin)	3.29E-04	2.012	5.51	35,964	236	5	14.8
3580	O00264	Membrane-associated progesterone receptor component 1	1.56E-03	2.353	4.56	21,641	147	3	21.6
3625	P26038	Moesin	1.56E-03	2.140	6.09	67,761	470	11	13.5
3626	P02545	Lamin-A/C	5.76E-04	2.114	6.57	74,380	836	15	28.2
3718	Q96CX2	BTB/POZ domain-containing protein KCTD12 (Pfetin)	1.65E-04	2.395	5.51	35,964	378	7	22.8
3727	Q96CX2	BTB/POZ domain-containing protein KCTD12 (Pfetin)	1.65E-04	2.668	5.51	35,964	352	6	20.9
3742	Q96CX2	BTB/POZ domain-containing protein KCTD12 (Pfetin)	8.23E-05	2.748	5.51	35,964	299	5	20.9
3756	Q96CX2	BTB/POZ domain-containing protein KCTD12 (Pfetin)	3.29E-04	2.806	5.51	35,964	445	9	28

(continued on next page)

Table 1 (continued)

Spots No [a]	Accession no [b]	Identified protein [b]	Wilcoxon test p value	Fold difference (ratio of means)	pI (cal) [c]	MW (cal) (kD) [c]	Protein score [d]	Peptide matches	Sequence coverage (%)
3757	Q96CX2	BTB/POZ domain-containing protein KCTD12 (Pfetin)	6.31E-04	3.117	5.51	35,964	497	8	29.8
3829	Q96CX2	BTB/POZ domain-containing protein KCTD12 (Pfetin)	1.65E-04	2.463	5.51	35,964	294	5	17.5

[a] Spot numbers refer to those in Fig. 1A.
[b] Accession numbers of proteins were derived from Swiss-Prot and NCBI nonredundant databases.
[c] Theoretical isoelectric point and molecular weight obtained from Swiss-Prot.
[d] Mascot score for the identified proteins based on the peptide ions score ($p<0.05$) (http://www.matrixscience.com).

(Fig. 3B and C). In our previous study, we compared the primary tumor proteome of GIST by 2D-DIGE with a small format gel. With less stringent criteria ($p<0.01$), we identified 25 gene products as being associated with outcomes. They included eight gene products identified employing the same criteria as in this study. Among the eight, four (endoplasmin, heat shock protein beta-1, lamin B1 and leukocyte elastase inhibitor) were not detected in this study, while the other four (pfetin, ATP-dependent RNA helicase DDX-39, superoxide dismutase and actin) were observed in both studies. The association between pfetin expression and prognosis in GIST was extensively examined [9], and the expression of superoxide dismutase was shown to correlate with malignant behaviors of various cancers [21]. In contrast, there have been no reports linking the expression of ATP-dependent RNA helicase DDX-39 to poor outcomes of cancer patients. Thus, we focused on the expression of ATP-dependent RNA helicase DDX-39.

We performed SDS-PAGE/Western blotting to validate different expressions of the identified proteins in the primary tumor tissues before treatments (Fig. 4A), and found that ATP-dependent RNA helicase DDX-39 showed results consistent with the 2D-DIGE data. Then, we immunohistochemically validated the association between the expression of ATP-dependent RNA helicase DDX39 in the primary tumor tissues and poor outcomes of GIST patients. Proteomics was achieved using the samples from cases at the National Cancer Center Hospital, and the immunohistochemical validation study was performed on samples from the newly enrolled cases at the Juntendo Hospital. In both cases, all patients in this study were not treated with any adjuvant therapy, and the expression of ATP-dependent RNA helicase DDX39 was not affected by any treatments. Immunohistochemistry showed diffuse staining of the nuclei of tumor cells with the antibody for ATP-dependent RNA helicase DDX39 (Fig. 4). High expression of ATP-dependent RNA helicase DDX39 was observed in the primary tumor tissues obtained from patients with poor outcomes (Upper panel, Fig. 4B), while weak expression of ATP-dependent RNA helicase DDX-39 was observed in the primary tumor tissues from patients with good outcomes (lower panel, Fig. 4B). These observations were consistent with the 2D-DIGE results.

In the additional 72 cases, Kaplan–Meier survival analysis revealed ATP-dependent RNA helicase DDX39 expression in the primary tumor tissues to correlate significantly and strongly with metastasis after surgery (Fig. 5A). The disease-free survival rate was 90.2% (21/72) for ATP-dependent RNA helicase DDX39-weak and 50.38% (51/72) for ATP-dependent RNA helicase DDX39-strong cases (Table 2). Univariate analysis demonstrated that disease-free survival period was statistically associated with the expression of ATP-dependent RNA helicase DDX39 ($p=0.0037$; log-rank test) as well as tumor size ($p=0.0064$) and risk classification ($p=0.006$) (Table 2). Multivariate analyses revealed that only ATP-dependent RNA helicase DDX39 expression was an independent significant predictor of disease-free survival ($p=0.047$; relative risk=3.186; 95% confidence interval, 1.015–10.006, Table 2).

We examined the prognostic values of ATP-dependent RNA helicase DDX39 in the two patient groups based on risk

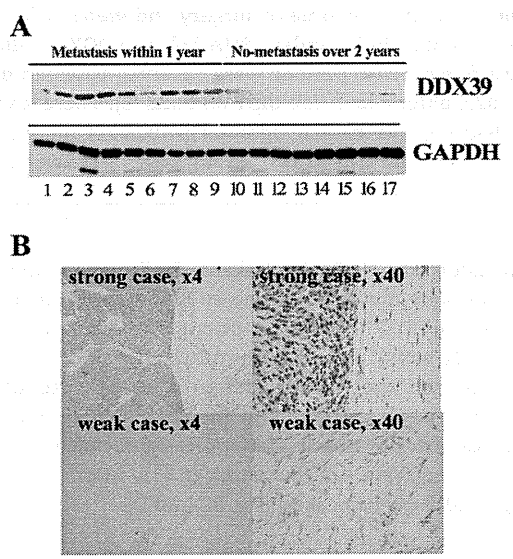

Fig. 4 – Validation of the differences in expressions of ATP-dependent RNA helicase DDX39 between groups. Samples from the GIST patients with poor outcomes expressed ATP-dependent RNA helicase DDX39 at significantly higher levels than those from patients with better outcomes. A. Western blotting. Case numbers correspond to those in Fig. 3. B. Immunohistochemistry; ATP-dependent RNA helicase DDX39 is overexpressed in samples from the GIST patients with poor outcomes(top, strong case), whereas it is underexpressed in those with better outcomes (bottom, weak case). ATP-dependent RNA helicase DDX39 localized in the nucleus in all cells.

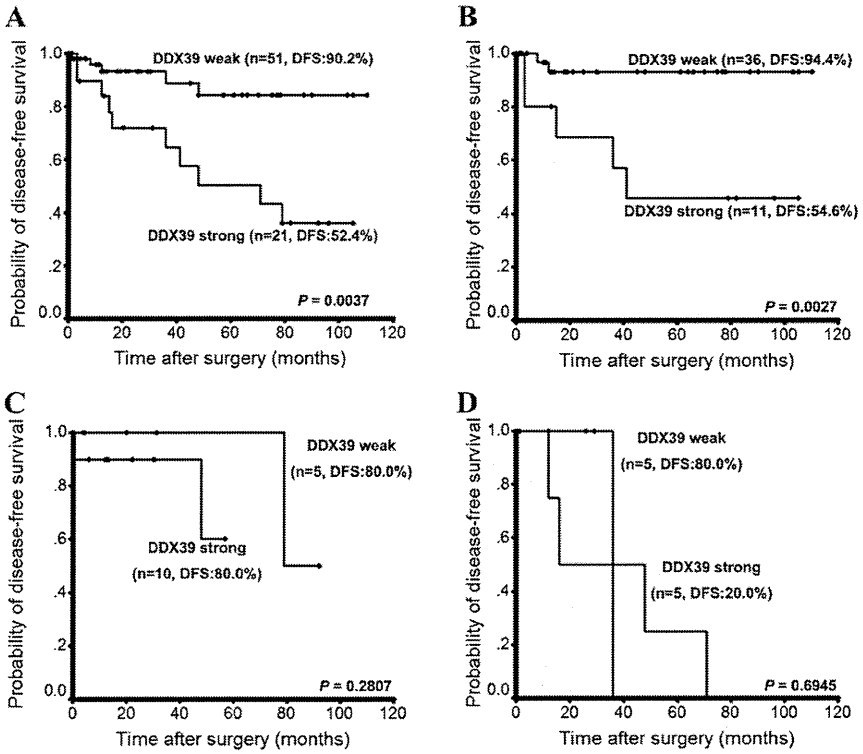

Fig. 5 – Relationship between disease-free survivals of GIST patients and the expression of ATP-dependent RNA helicase DDX39. (A) Kaplan–Meier survival curve demonstrated the relationship between the expression of ATP-dependent RNA helicase DDX39 at the time of surgery and metastasis after surgery for 72 GIST patients; the groups with strong and weak expression of ATP-dependent RNA helicase DDX39 differed significantly (p=0.0037).Statistically significant differences in disease-free survival periods were observed between the ATP-dependent RNA helicase DDX39-strong and weak subgroups (p=0.0027) among low-risk GIST patients (B). There was marginal differences between the ATP-dependent RNA helicase DDX39-strong and weak subgroups (p=0.0027) among intermediate- (C) and high-risk GIST patients (D) with no statistical significances. The criteria for "strong case" and "weak case" were described in Fig. 4B.

classification (Fig. 5B–D). Remarkable findings were that low-risk cases were divided into two subgroups, ATP-dependent RNA helicase DDX39-weak and -strong, with the latter having significantly worse outcomes (p=0.0027) (Fig. 5B). The differences between the ATP-dependent RNA helicase DDX39-strong and -weak subgroups in the intermediate and high-risk cases did not reach statistical significance, probably because there were too few cases (n=15, intermediate-risk cases; n=10, high-risk cases) (Fig. 5C and D).

4. Discussion

Because adjuvant molecular targeting therapy using imatinib mesylate (STI571, Novartis)was proven to be effective for treating GIST patients [3], and 60% to 80%of GIST patients can be cured by surgical resection alone [1,2], biomarkers to predict the metastasis after surgery have long been desired in GIST. Statistically enough number of clinical samples with well-organized clinicopathological data, established proteomics modalities and independent validation samples are essentially required for biomarker studies. However, the number of an initial sample set is often limited in the case the frozen tissues are required for proteomics, and the validation studies are the rate limiting step of biomarker studies. GIST is characterized by mutations of c-kit and platelet derived growth factor receptor (PDGFR) [3], suggesting that the GIST cells may have relatively similar molecular profiles. If the molecular backgrounds of GIST are relatively rare, it may be possible to develop biomarkers even starting with a small number of samples. In this study, we detected ATP-dependent RNA helicase DDX39 in 17 samples, and successfully validate its prognostic value in the additional 72 cases. In our experience, biomarker studies with a small number of initial samples often failed at the validation phase. These successful results may be attributable to relatively homogenous molecular backgrounds of GIST cells.

ATP-dependent RNA helicase DDX39 was originally reported as a novel growth-associated RNA helicase [22]. Overexpression of ATP-dependent RNA helicase DDX39 was observed in lung squamous cell carcinoma, and up-regulation of this enzyme stimulated colony formation [23]. Recently, Yoo et al. reported that ATP-dependent RNA helicase DDX39 was required for global genome integrity as well as telomere protection [24]. They found that overexpression

Table 2 – Univariate and multivariate analyses, and the relationships between RNA helicase DDX39 and clinicopathological variables.

Variable	Number of cases	DDX39 strong	DDX39 weak	Correlation (DDX39) χ^2 P value	Disease-free survival		Multivariate analysis of disease-free survival by Cox regression		
					Rate (%)	Log-rank (P value)	P value	Relative risk	95% confidence interval
Age									
<60	34	11	23	0.38	76.47	0.444			
≥60	38	10	28		81.58				
Sex									
F	26	5	21	0.13	73.91	0.241			
M	46	16	30		88.46				
Site									
Stomach	53	18	35	0.251	79.25	0.4869			
Small intestine	16	2	14		81.25				
Other	3	1	2		66.67				
Histology									
Spindle	63	17	46	0.082	80.95	0.8071			
Epithelioid	7	2	5		71.43				
Mixed	2	2	0		50				
Size (cm)									
<5	46	11	35	0.222	86.96	0.0064	0.501	1.599	0.407–6.277
5–15	23	8	15		73.91				
≥15	3	2	1		0				
Necrosis									
Present	16	5	11	0.531	80.36	0.4567			
Absent	56	16	40		75				
Risk classification[a]									
Low	47	11	36	0.225	85.11	0.006	0.686	1.271	0.397–4.072
Intermediate	15	5	10		80				
High	10	5	5		50				
DDX39[b]									
Strong	21	21	0		90.2	0.0037	0.047	3.186	1.015–10.006
Weak	51	0	51		52.38				

[a] Risk classification based on tumor size and MIB-1 grade (11).
[b] Criteria for immunohistochemical staining a strong and weak DX39 referred to those in Fig. 4.

of ATP-dependent RNA helicase DDX39 in telomerase-positive human cancer cells led to progressive telomere elongation, and depletion of endogenous ATP-dependent RNA helicase DDX39 by small hairpin RNA, resulting in telomere shortening [24]. All of these observations predicted the associations of ATP-dependent RNA helicase DDX39 with poor clinical outcomes of cancer patients, but the present study is the first to demonstrate the prognostic significance of ATP-dependent RNA helicase DDX39 in GIST, employing a proteomic approach.

In this study, we identified the associations of 25 unique gene products with the outcomes of GIST patients, and examined ATP-dependent RNA helicase DDX-39. The possible utilities of the other proteins should be addressed in future studies. The discrepancy between the data obtained by the different 2D gel formats may be attributable to differing resolutions and focusing of protein spots. As we used the same sample set as in our previous study [9], the long storage period might also have affected the results of the proteome study.

Previous clinical studies demonstrated tyrosine kinase inhibitors to reduce metastasis after GIST resection, and prognostic modalities identifying patients not curable by surgery alone are thus needed [25]. However, there is no established prognostic molecular biomarker in GIST. The previously reported biomarkers included p16 [7,26–29], p53 [30,31], COX2 [30,32], IGF [33], Bcl-2 [34,35], SKP2 [36], P21WAF2 [37], Bax [37], RKIP [38], CD44 [39,40], CD26 [41], L1 (CD171) [42] and pfetin [9,43,44]. We showed that ATP-dependent RNA helicase DDX39 was a novel independent prognostic biomarker, whose expression was most significantly associated with poor prognosis in GIST patients, among the established clinico-pathological parameters (Table 2). Further multi-institutional validation studies for these biomarkers considering low incidence of GIST [1,2] will lead a prognostic modality for GIST patients.

Supplementary materials related to this article can be found online at doi:10.1016/j.jprot.2011.10.005.

Acknowledgments

This work was supported by a grant from the Ministry of Health, Labor and Welfare and by the Program for Promotion of Fundamental Studies in Health Sciences of the National Institute of Biomedical Innovation of Japan, to Tadashi Kondo. The antibody against ATP-dependent RNA helicase DDX-39 was provided from BioMatrix Research Institute.

REFERENCES

[1] Joensuu H, Kindblom LG. Gastrointestinal stromal tumors—a review. Acta Orthop Scand Suppl 2004;75:62–71.
[2] Miettinen M, El-Rifai W, HLS L, Lasota J. Evaluation of malignancy and prognosis of gastrointestinal stromal tumors: a review. Hum Pathol 2002;33:478–83.
[3] Dematteo RP, Owzar K, Maki R. Adjuvant imatinib mesylate increases recurrence free survival (RFS) in patients with completely resected localized primary gastrointestinal stromal tumor (GIST). 2007. North American Intergroup Phase III trial ACOSOG Z9001. J Clin Oncol, ASCO Annual Meeting Proceedings 2007;25:10079.
[4] Heinrich MC, Corless CL, Blanke CD, Demetri GD, Joensuu H, Roberts PJ, et al. Molecular correlates of imatinib resistance in gastrointestinal stromal tumors. J Clin Oncol 2006;24:4764.
[5] Debiec-Rychter M, Dumez H, Judson I, Wasag B, Verweij J, Brown M, et al. Use of c-KIT/PDGFRA mutational analysis to predict the clinical response to imatinib in patients with advanced gastrointestinal stromal tumours entered on phase I and II studies of the EORTC Soft Tissue and Bone Sarcoma Group. Eur J Cancer 2004;40:689–95.
[6] Debiec-Rychter M, Sciot R, Le Cesne A, Schlemmer M, Hohenberger P, van Oosterom AT, et al. KIT mutations and dose selection for imatinib in patients with advanced gastrointestinal stromal tumours. Eur J Cancer 2006;42: 1093–103.
[7] Schneider-Stock R, Boltze C, Lasota J, Miettinen M, Peters B, Pross M, et al. High prognostic value of p16INK4 alterations in gastrointestinal stromal tumors. J Clin Oncol 2003;21: 1688–97.
[8] Schneider-Stock R, Boltze C, Lasota J, Peters B, Corless CL, Ruemmele P, et al. Loss of p16 protein defines high-risk patients with gastrointestinal stromal tumors: a tissue microarray study. AACR 2005:638–45.
[9] Suehara Y, Kondo T, Seki K, Shibata T, Fujii K, Gotoh M, et al. Pfetin as a prognostic biomarker of gastrointestinal stromal tumors revealed by proteomics. Clin Cancer Res 2008;14:1707–17.
[10] LA Stankey RH. Pathology and genetics of tumours of the digestive system. Lyon: IARC Press; 2000.
[11] Hasegawa T, Matsuno Y, Shimoda T, Hirohashi S. Gastrointestinal stromal tumor: consistent CD117 immunostaining for diagnosis, and prognostic classification based on tumor size and MIB-1 grade. Hum Pathol 2002;33: 669–76.
[12] Unlu M, Morgan ME, Minden JS. Difference gel electrophoresis: a single gel method for detecting changes in protein extracts. Electrophoresis 1997;18:2071–7.
[13] Yokoo H, Kondo T, Fujii K, Yamada T, Todo S, Hirohashi S. Proteomic signature corresponding to alpha fetoprotein expression in liver cancer cells. Hepatology 2004;40:609–17.
[14] Suehara Y, Kondo T, Fujii K, Hasegawa T, Kawai A, Seki K, et al. Proteomic signatures corresponding to histological classification and grading of soft-tissue sarcomas. Proteomics 2006;6:4402–9.
[15] Kondo T, Hirohashi S. Application of highly sensitive fluorescent dyes (CyDye DIGE Fluor saturation dyes) to laser microdissection and two-dimensional difference gel electrophoresis (2D-DIGE) for cancer proteomics. Nat Protoc 2007;1:2940–56.
[16] Kaplan E. Nonparametric estimation from incomplete observations. J Am Stat Assoc 1958;53:457–81.
[17] Cox D. Regression models and life table. J R Stat Soc 1972;34: 187–220.
[18] Voris BP, Young DA. Very-high-resolution two-dimensional gel electrophoresis of proteins using giant gels. Anal Biochem 1980;104:478–84.
[19] Campostrini N, Areces LB, Rappsilber J, Pietrogrande MC, Dondi F, Pastorino F, et al. Spot overlapping in two-dimensional maps: a serious problem ignored for much too long. Proteomics 2005;5:2385–95.
[20] Alban A, David SO, Bjorkesten L, Andersson C, Sloge E, Lewis S, et al. A novel experimental design for comparative two-dimensional gel analysis: two-dimensional difference gel electrophoresis incorporating a pooled internal standard. Proteomics 2003;3:36–44.
[21] Kinnula VL, Crapo JD. Superoxide dismutases in malignant cells and human tumors. Free Radic Biol Med 2004;36:718–44.
[22] Sugiura T, Sakurai K, Nagano Y. Intracellular characterization of DDX39, a novel growth-associated RNA helicase. Exp Cell Res 2007;313:782–90.
[23] Sugiura T, Nagano Y, Noguchi Y. DDX39, upregulated in lung squamous cell cancer, displays RNA helicase activities and promotes cancer cell growth. Cancer Biol Ther 2007;6:957–64.
[24] Yoo HH, Chung IK. Requirement of DDX39 DEAD box RNA helicase for genome integrity and telomere protection. Aging Cell 2011;10:557–71.
[25] Dematteo RP, Ballman KV, Antonescu CR, Maki RG, Pisters PW, Demetri GD, et al. Adjuvant imatinib mesylate after resection of localised, primary gastrointestinal stromal tumour: a randomised, double-blind, placebo-controlled trial. Lancet 2009;373:1097–104.
[26] Huang HY, Huang WW, Lin CN, Eng HL, Li SH, Li CF, et al. Immunohistochemical expression of p16INK4A, Ki-67, and Mcm2 proteins in gastrointestinal stromal tumors: prognostic implications and correlations with risk stratification of NIH consensus criteria. Ann Surg Oncol 2006;13:1633–44.
[27] Schmieder M, Wolf S, Danner B, Stoehr S, Juchems MS, Wuerl P, et al. p16 expression differentiates high-risk gastrointestinal stromal tumor and predicts poor outcome. Neoplasia 2008;10:1154–62.
[28] Schneider-Stock R, Boltze C, Lasota J, Peters B, Corless CL, Ruemmele P, et al. Loss of p16 protein defines high-risk patients with gastrointestinal stromal tumors: a tissue microarray study. Clin Cancer Res 2005;11:638–45.
[29] Steigen SE, Bjerkehagen B, Haugland HK, Nordrum IS, Loberg EM, Isaksen V, et al. Diagnostic and prognostic markers for gastrointestinal stromal tumors in Norway. Mod Pathol 2008;21:46–53.
[30] Gumurdulu D, Erdogan S, Kayaselcuk F, Seydaoglu G, Parsak CK, Demircan O, et al. Expression of COX-2, PCNA, Ki-67 and p53 in gastrointestinal stromal tumors and its relationship with histopathological parameters. World J Gastroenterol 2007;13:426–31.
[31] Neves LR, Oshima CT, Artigiani-Neto R, Yanaguibashi G, Lourenco LG, Forones NM. Ki67 and p53 in gastrointestinal stromal tumors—GIST. Arq Gastroenterol 2009;46:116–20.
[32] Turkoz HK, Alkan I, Sisman S, Ozcan D. Cyclooxygenase-2 expression and connection with tumor recurrence and

histopathologic parameters in gastrointestinal stromal tumors. APMIS 2009;117:825–30.
[33] Braconi C, Bracci R, Bearzi I, Bianchi F, Sabato S, Mandolesi A, et al. Insulin-like growth factor (IGF) 1 and 2 help to predict disease outcome in GIST patients. Ann Oncol 2008;19:1293–8.
[34] Meara RS, Cangiarella J, Simsir A, Horton D, Eltoum I, Chhieng DC. Prediction of aggressiveness of gastrointestinal stromal tumours based on immunostaining with bcl-2, Ki-67 and p53. Cytopathology 2007;18:283–9.
[35] Steinert DM, Oyarzo M, Wang X, Choi H, Thall PF, Medeiros LJ, et al. Expression of Bcl-2 in gastrointestinal stromal tumors: correlation with progression-free survival in 81 patients treated with imatinib mesylate. Cancer 2006;106:1617–23.
[36] Di Vizio D, Demichelis F, Simonetti S, Pettinato G, Terracciano L, Tornillo L, et al. Skp2 expression is associated with high risk and elevated Ki67 expression in gastrointestinal stromal tumours. BMC Cancer 2008;8:134.
[37] Liu FY, Qi JP, Xu FL, Wu AP. Clinicopathological and immunohistochemical analysis of gastrointestinal stromal tumor. World J Gastroenterol 2006;12:4161–5.
[38] Martinho O, Gouveia A, Silva P, Pimenta A, Reis RM, Lopes JM. Loss of RKIP expression is associated with poor survival in GISTs. Virchows Arch 2009;455:277–84.
[39] Hsu KH, Tsai HW, Shan YS, Lin PW. Significance of CD44 expression in gastrointestinal stromal tumors in relation to disease progression and survival. World J Surg 2007;31: 1438–44.
[40] Montgomery E, Abraham SC, Fisher C, Deasel MR, Amr SS, Sheikh SS, et al. CD44 loss in gastric stromal tumors as a prognostic marker. Am J Surg Pathol 2004;28:168–77.
[41] Yamaguchi U, Nakayama R, Honda K, Ichikawa H, Hasegawa T, Shitashige M, et al. Distinct gene expression-defined classes of gastrointestinal stromal tumor. J Clin Oncol 2008;26:4100–8.
[42] Kaifi JT, Strelow A, Schurr PG, Reichelt U, Yekebas EF, Wachowiak R, et al. L1 (CD171) is highly expressed in gastrointestinal stromal tumors. Mod Pathol 2006;19:399–406.
[43] Kikuta K, Gotoh M, Kanda T, Tochigi N, Shimoda T, Hasegawa T, et al. Pfetin as a prognostic biomarker in gastrointestinal stromal tumor: novel monoclonal antibody and external validation study in multiple clinical facilities. Jpn J Clin Oncol 2010;40:60–72.
[44] Kubota D, Orita H, Yoshida A, Gotoh M, Kanda T, Tsuda H, et al. Pfetin as a prognostic biomarker for gastrointestinal stromal tumor: validation study in multiple clinical facilities. Jpn J Clin Oncol 2011;41:1194–202.

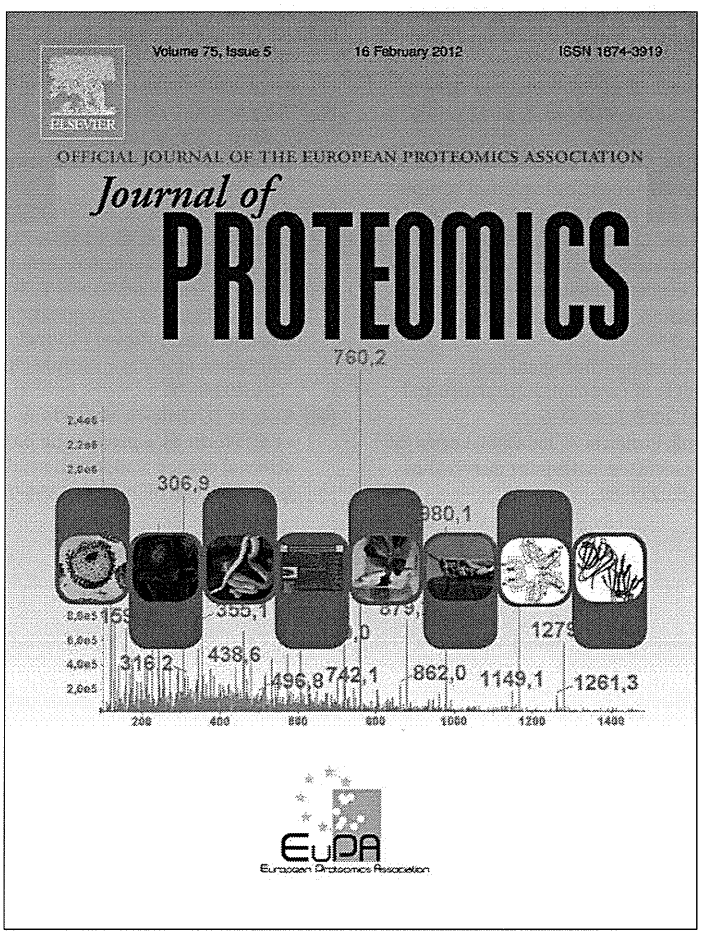

JOURNAL OF PROTEOMICS 75 (2012) 1577–1589

Available online at www.sciencedirect.com

SciVerse ScienceDirect

www.elsevier.com/locate/jprot

Macrophage-capping protein as a tissue biomarker for prediction of response to gemcitabine treatment and prognosis in cholangiocarcinoma

Noriaki Morofuji[a,g], *Hidenori Ojima*[b], *Hiroaki Onaya*[c], *Takuji Okusaka*[d], *Kazuaki Shimada*[e], *Yoshihiro Sakamoto*[e], *Minoru Esaki*[e], *Satoshi Nara*[e], *Tomoo Kosuge*[e], *Daisuke Asahina*[f], *Masahiko Ushigome*[f], *Nobuyoshi Hiraoka*[b], *Masato Nagino*[g], *Tadashi Kondo*[a,*]

[a]*Division of Pharmacoproteomics, National Cancer Center Research Institute, Tokyo, Japan*
[b]*Pathology Division, National Cancer Center Research Institute, Tokyo, Japan*
[c]*Diagnostic Radiology Section, Clinical Trials and Practice Support Division, Center for Cancer Control and Information Services, National Cancer Center, Tokyo, Japan*
[d]*Hepatobiliary and Pancreatic Oncology Division, National Cancer Center Hospital, Tokyo, Japan*
[e]*Hepatobiliary and Pancreatic Surgery Division, National Cancer Center Hospital, Tokyo, Japan*
[f]*Pathology Division, National Cancer Center Hospital, Tokyo, Japan*
[g]*Division of Surgical Oncology, Department of Surgery, Nagoya University Graduate School of Medicine, Nagoya, Japan*

ARTICLE INFO

Article history:
Received 13 August 2011
Accepted 24 November 2011
Available online 6 December 2011

Keywords:
Cholangiocarcinoma
Gemcitabine
Biomarker
Two-dimensional difference gel electrophoresis
Macrophage-capping protein (CapG)

ABSTRACT

Cholangiocarcinoma is one of the deadliest malignancies worldwide. Recent studies reported that treatment with gemcitabine was effective in prolonging survival. However, as the treatment only benefited a limited subset of patients, selection of patients before treatment is required. To discover biomarkers predictive of the response to gemcitabine treatment in cholangiocarcinoma, we examined the proteome of three types of material resource; ten cell lines, nine xenografts and nine surgically resected primary tumors from patients who exhibited different response to gemcitabine treatment. Two-dimensional difference gel electrophoresis generated quantitative protein expression profiles including 3571 protein spots. We detected 172 protein spots with significant correlation with response to gemcitabine treatment. All proteins corresponding to these 172 protein spots were identified by mass spectrometry. We found that the macrophage-capping protein (CapG) was associated with response to gemcitabin treatment in all three types of material source. Immunohistochemical validation in an additional set of 196 cholangiocarcinoma cases revealed that CapG expression was associated with lymphatic invasion status and overall survival. Multivariate analysis showed that CapG protein expression was an independent prognostic factor for overall survival. In conclusion, CapG was identified as a novel candidate biomarker to predict response to gemcitabine treatment and survival in cholangiocarcinoma.

* *Corresponding author at:* Division of Pharmacoproteomics, National Cancer Center Research Institute, 5-1-1 Tsukiji, Chuo-ku, Tokyo 104-0045, Japan. Tel.: +81 3 3542 2511x3004; fax: +81 3 3547 5298.
E-mail address: takondo@ncc.go.jp (T. Kondo).

1874-3919/$ – see front matter © 2011 Elsevier B.V. All rights reserved.
doi:10.1016/j.jprot.2011.11.030

1. Introduction

Cholangiocarcinoma is one of the leading causes of cancer death, the incidence of which is rising worldwide [1–3]. Cholangiocarcinoma is classified into the intra- and extrahepatic types, both having poor clinical outcome; the 5-year survival rate after resection is 8–47% and 20–54% for intra- and extrahepatic cholangiocarcinoma (IHCC and EHCC) respectively [4]. Previous studies have reported that surgical resection is the only curative treatment [5–8], and no standard chemotherapy regimen has been established for inoperable or recurrent cases after surgical resection.

Gemcitabine (GEM, 2′-deoxy-2′-difluorodeoxycytidine: Gemzar, Eli Lilly, Indianapolis, IL), a deoxycytidine analog with structural and metabolic similarities to cytarabine, has been reported to benefit patients with unresectable, locally advanced or metastatic adenocarcinoma, and has been considered as a first-line chemotherapy for cholangiocarcinoma [1]. However, in cholangiocarcinoma, response rates for gemcitabine treatment range from 8 to 36%, and the median survival period of the patients subjected to gemcitabine treatment ranges from 6.3 to 16 months [1]. These observations suggest that certain molecular variables may exist that explain the different response to GEM treatment in cholangiocarcinoma. The identification of biomarkers predictive of the patients' response to GEM treatment will allow selective use of gemcitabine and is urgently needed in practice. To date, however, there has been no attempt to clarify the molecular mechanisms of the varying response to GEM treatment in cholangiocarcinoma.

The proteome is a functional translation of the genome directly regulating cancer phenotypes, and cancer proteomics has revealed the molecular background of carcinogenesis and cancer progression of a range of tumor types. Proteomic studies have identified biomarker candidates and possible therapeutic targets in hepatocellular carcinoma [9,10], cholangiocarcinoma [11,12], and pancreatic cancer [13,14]. However, proteomic tools have not yet been employed to develop biomarkers predictive of the efficacy of GEM treatment in any type of malignancy, probably because of the difficulty in obtaining suitable clinical material.

In this report, we investigated the proteomic features corresponding to the response to GEM treatment in cholangiocarcinoma in three types of material resource; the proteome of cell lines, tumor xenografts and primary tumors from cholangiocarcinoma patients who exhibited different response to GEM treatment were examined by two-dimensional difference gel electrophoresis (2D-DIGE) [15]. As a result, macrophage-capping protein (CapG) was identified as a biomarker candidate predictive of the efficacy of GEM treatment. The prognostic performance of CapG was confirmed by immunohistochemistry in an additional set of 196 cholangiocarcinoma cases. This is the first report concerning the predictive and prognostic value of CapG expression in cholangiocarcinoma. By measuring CapG expression in primary tumors, we will be able to optimize current therapeutic strategies for patients with cholangiocarcinoma.

2. Materials and methods

We examined the protein expression profiles of ten cholangiocarcinoma cell lines, nine xenografts and nine surgically resected tissues from patients who exhibited different response to gemcitabine treatment.

2.1. Cell lines

Ten human cholangiocarcinoma cell lines were included in this study (Table 1). Six cell lines, NCC-CC1, NCC-CC3-1, NCC-CC3-2, NCC-CC4-1, NCC-BD1 and NCC-BD2, were established in the National Cancer Center Research Institute [16]. TKKK and TGBC24TKB were purchased from RIKEN Bio Resource Center (Tsukuba, Japan), and OZ and HuCCT1 from the Japanese Collection of Research Bioresources (Osaka, Japan). The TKKK, NCC-CC1, NCC-CC3-1, NCC-CC3-2, and NCC-CC4-1 cell lines were derived from IHCC, while the OZ, TGBC24TKB, HuCCT1, NCC-BD1 and NCC-BD2 cell lines from EHCC [16]. These cell lines were classified into the sensitive and resistant group based on their 50% inhibition (IC50) value for GEM according to our previous report [16]. The protein expression profiles of these cell lines were generated. Cell pellets were embedded in paraffin blocks for immunohistochemistry.

2.2. Xenografts

Cells from all cell lines were subcutaneously implanted in 5–7 weeks old congenital athymic female C.B17/Icr-scid (scid/scid) mice (CLEA Japan, Tokyo). The mice were sacrificed when tumor size reached 1–2 cm in diameter. As implantation of NCC-BD2 cells did not result in the development of tumors, samples from nine xenografts were used in the proteomic study (Table 1). The xenografts were grouped in two groups according to the characteristics of the cell lines from which they derived; xenografts from the GEM-sensitive (GEM-sensitive xenografts) and GEM-resistant (GEM-resistant xenograft) cell lines. The resected xenografts were cut into 2–4 mm^3 pieces, snap-frozen in liquid nitrogen, and stored at −80 °C until use. The recovered specimens were histologically examined by a certified pathologist (H.O.) [16].

Mice were kept at the Animal Care and Use Facilities of the National Cancer Center (Tokyo, Japan) under specific pathogen-free conditions. All experiments were approved by the Animal Care and Ethical Review Board of the National Cancer Center.

2.3. Case selection

Among the 100 patients who underwent surgery for cholangiocarcinoma between September 2003 and October 2007, 34 patients had recurrence and received chemotherapy, and were followed up for at least six months. Among these 34 patients, the 24 patients who were treated with GEM were initially selected for the study. The median follow-up period in these 24 patients was 498 days. A further 15 of these cases were excluded because: (1) the drug administration period was less than one month (three cases), (2) there was disagreement on the diagnosis of tumor recurrence offered between the oncologist (T.O.) and radiologist (H.O.) (three cases), (3) the efficacy of GEM treatment was not evaluated adequately (five cases), (4) the histological diagnosis was that of an uncommon type of carcinoma (bile duct cystadenocarcinoma, solid adenocarcinoma and combined carcinoma) in three

Table 1 – Characteristics of samples.

Cell lines

Sample number [a]	Cell line name [b]	Origin of cell lines [b]	Drug sensitivity [c]	Xenograft [d]
1	TGBC24TKB	RIKEN Bio Resouce Center, EHCC	Sensitive	26
2	Hucct1	Japanese Collection of Research Bioresources, EHCC	Sensitive	25
3	TKKK	RIKEN Bio Resouce Center, IHCC	Resistant	31
4	OZ	Japanese Collection of Research Bioresources, EHCC	Resistant	27
5	NCC-CC1	National Cancer Center, IHCC	Resistant	32
6	NCC-BD1	National Cancer Center, EHCC	Sensitive	28
7	NCC-CC3-2	National Cancer Center, IHCC	Sensitive	30
8	NCC-CC4-1	National Cancer Center, IHCC	Sensitive	33
9	NCC-BD2	National Cancer Center, EHCC	Resistant	–
10	NCC-CC3-1	National Cancer Center, IHCC	Sensitive	29

Xenografts

Sample number [a]	Name of cell line [e]	Drug sensitivity [f]
25	Hucct1	Sensitive
26	TGBC24TKB	Sensitive
27	OZ	Resistant
28	NCC-BD1	Sensitive
29	NCC-CC3-1	Sensitive
30	NCC-CC3-2	Sensitive
31	TKKK	Resistant
32	NCC-CC1	Resistant
33	NCC-CC4-1	Sensitive

Primary tumors with recurrence that underwent gemcitabine therapy after surgery

Sample number [a]	Patient age	Patient gender	Pathological diagnosis [g]	Histologic type [h]	TNM stage [i]		Duration of SD (month) [j]
34	72	Female	Upper BDCa	Adeno/mod	pT4N1M0	III	0.20
35	48	Male	Hilar BDCa	Adeno/well	pT3N1M0	IIB	3.67
36	60	Male	Entire BDCa	Pap	pT2N0M0	II	1.43
38	61	Male	Middle BDCa	Adeno/mod	pT3N1M0	IIB	6.83
39	67	Male	Lower BDCa	Adeno/mod	pT3N1M0	IIB	8.33
40	75	Male	CCC	Adeno/mod	pT3N0M0	IIIA	10.30
41	68	Male	CCC	Adeno/mod	pT4N0M0	IIIB	7.60
43	50	Male	CCC	Adeno/mod	pT1N0M0	I	6.23
44	72	Male	Lower BDCa	Adeno/mod	pT2N0M0	IB	3.67

[a] Sample numbers correspond to those in GeMDBJ Proteomics (https://gemdbj.nibio.go.jp/dgdb/DigeTop.do).
[b] The characteristics of cell lines were described in our previous paper (16). IHCC, intrahepatic cholangiocarcinoma; EHCC, extrahepatic cholangiocarcinoma.
[c] The *in vitro* assay for determining the sensitivity of the treatment with gemcitabine was detailed in our previous paper (16).
[d] These xenografts were made following transplantation of cell line material. Sample numbers correspond to those in GeMDBJ Proteomics (https://gemdbj.nibio.go.jp/dgdb/DigeTop.do).
[e] These cell lines provided the material used for transplantation.
[f] Determining the sensitivity was based on the drug sensitivity of the original cell lines.
[g] CCC, Cholangiocellular carcinoma; Upper BDCa, Upper third of extrahepatic bile duct carcinoma; Hilar BDCa, Hilar Bile duct carcinoma; Entire BDCa, Entire extrahepatic bile duct carcinoma; Middle BDCa, Middle third of extrahepatic bile duct carcinoma; Lower BDCa, Lower third of extrahepatic bile duct carcinoma.
[h] Adeno, Adenocarcinoma; mod, moderately differentiated; well, well differentiated; Pap, Papillary adenocarcinoma; Muc, Mucinous adenocarcinoma.
[i] TNM Classification of Malignant Tumours, Sobin LH, Wittekind Ch (eds): International Union Against Cancer (UICC): "TNM classification of malignant tumors". 6th ed. New York: Wiley; 2002 (18).
[j] The duration of the period in which the disease was stable (SD) after treatment with gemcitabine.

cases, (5) preoperative radiation therapy had been performed in one patient. Finally, nine cases met all the criteria and were subjected to the proteomic study (Table 1). The effects of chemotherapy were assessed by an oncologist (T.O.) and a radiologist (H.O.) in accordance with the chemotherapy response evaluation criteria in solid tumors (RECIST) guidelines [17]. None of the nine patients was judged as showing a complete response (CR) or a partial response (PR). The patients were grouped into the effective or non-effective group. The "effective" group included five patients whose disease state was judged as stable (SD) for more than six months during chemotherapy. The "non-effective" group included four patients whose disease state was judged as stable (SD) for less than six months, or as progressive (PD) during chemotherapy.

The expression of CapG was evaluated in an additional set of 196 patients with cholangiocarcinoma who underwent initial surgical resection between February 1990 and June 2004 at the National Cancer Center Hospital. No patients in this study received any preoperative therapy. The clinicopathological features of the patients are listed in Supplementary Table 1. Tumors were classified according to the International Union against Cancer tumor-node-metastasis (TNM) classification [18]. This study was approved by the Ethical Review Board of the National Cancer Center, and informed consent was obtained from all patients in this study.

2.4. *Laser microdissection*

As cholangiocarcinoma tissues are rich in stroma cells, laser microdissection was performed to recover pure populations of tumor cells [15,19] (Fig. 1A). In brief, 10 μm thick frozen sections were prepared from tumor tissues and stained with hematoxylin and eosin (HE) or hematoxylin alone. The cells were recovered under microscopic observation with the use of ultraviolet laser (MMI CellCut; Molecular Machines & Industries, Glattburg, Switzerland). One mm^2 area of tumor tissue (~3000 cells) was recovered for each 2D-DIGE gel image. The proteins were extracted from the recovered tissues using a urea lysis buffer containing 6 M urea, 2 M thiourea, 3%{3-[(3-cholamidopropyl)dimethylammonio]-1-propane-sulfonate}, and 1% Triton X-100, and stored at −80 °C until use.

2.5. *2D-DIGE and image analysis*

2D-DIGE was performed as previously described [15,19]. In brief, a common internal control sample was created by mixing a small portion of all protein samples used in this study, and labeled with Cy3 fluorescent dye (CyDye DIGE Fluor saturation dye, GE Healthcare Biosciences, Uppsala, Sweden). Individual samples were labeled with Cy5 fluorescent dye (CyDye DIGE Fluor saturation dye, GE Healthcare Biosciences). These differently labeled protein samples were mixed together, and separated by two-dimensional gel electrophoresis (2D-PAGE), according to the isoelectric point and molecular weight of the proteins (Fig. 1B). The first dimension separation was achieved using a 24 cm-length immobiline gel (IPG, pI 4–7, GE Healthcare Biosciences), while the second separation using a home-made gradient gel and GiantGelRunner (Biocraft, Tokyo, Japan), with

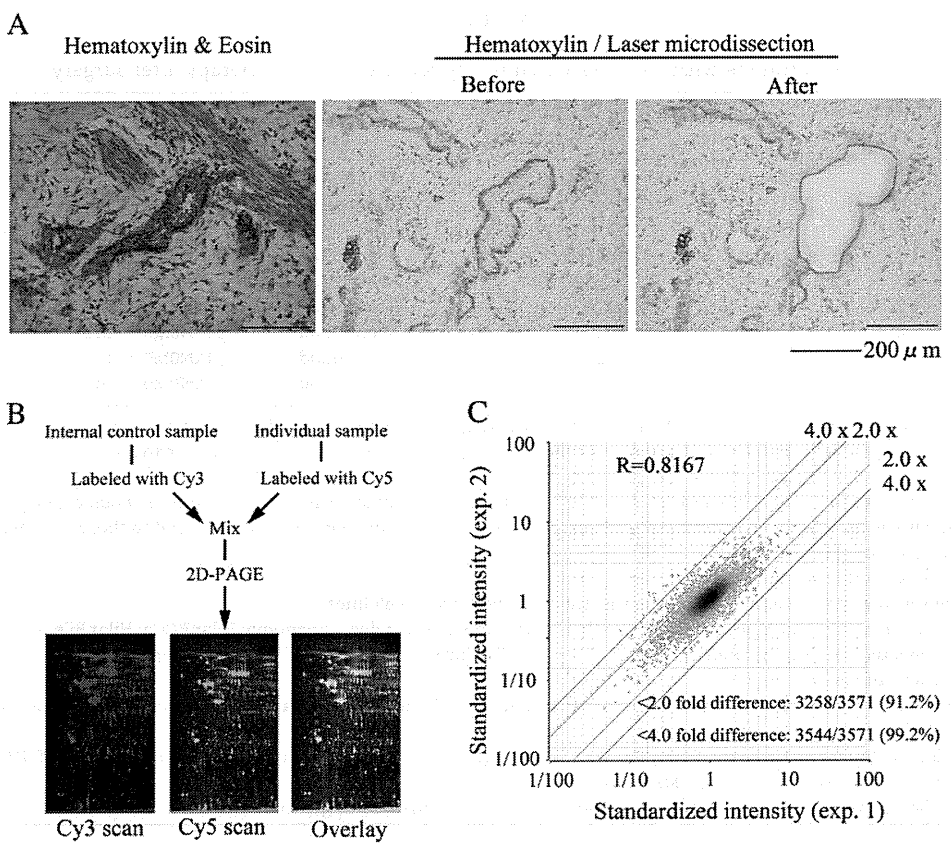

Fig. 1 – (A) Pure populations of tumor cells were recovered using laser microdissection to achieve accurate and cell-specific expression profiles. Tissue sections were stained with standard hematoxylin and eosin, and neighboring sections were stained with hematoxylin alone for laser microdissection. (B) The proteins extracted from laser microdissection tissues were labeled with fluorescent dyes. After mixing the internal control sample with the individual one, the protein samples were separated by 2D-PAGE. After gel electrophoresis, gel images were obtained by laser scanning. (C) Scatter graph demonstrating the high reproducibility of 2D-DIGE. The reproducibility was examined by running the identical sample, Sample 3 (Table 1), twice, and the intensities of all spot pairs were compared.